Cume #371

3 Question Categories; 65 Points Possible; 48 Points ($\simeq$ 75%) is Guaranteed Pass
passes below this score are still a possibility
Administered: April 21, 2012

The Multiphase Intergalactic Medium toward PKS 2155-304

J. M. Shull, J. Tumlinson, & M. L. Giroux (2003), ApJL 594, 107-110

Please start each question (by number) on a new sheet of paper, write on only one side of the paper, and staple them together in order of question number when finished. Please present your results in the order that the individual questions appear.

1. Some possibly useful physical constants are listed in Table 1.
2. A hand out of a blank graph is provided for Problem 3.
3. A hand out of the collisional ionization cooling function, $\Lambda(T, Z)$, is provided for Problem 4.

1. **[20 pts] Cosmic Hydrogen Density:**

   In § 1, the authors quote results from the literature that $\Omega_b = 0.02\,h^{-2}$, from which they deduce that the global co-moving hydrogen number density is $n_{\rm H} = 1.9 \times 10^{-7}$ cm^{-3}.

   (a) [4 pts] What is the definition of Ω_b? Write this definition down in symbolic form and provide a written definition of the terms.

   (b) [5 pts] If $\Omega_m = 0.27$ (the sum of baryonic and dark matter), compute the global mass fraction of baryons in the universe, f_b. Show your work.

   (c) [4 pts] From Ω_b, the author's compute ρ_b, the global co-moving baryonic density. Using this co-moving value, what is the global *proper* density at redshift $z = 0$? What is the global *proper* density at redshift $z = 3$?

   (d) [7 pts] From the global co-moving baryonic density ρ_b, the author's compute compute $n_{\rm H}$, the global co-moving hydrogen number density. They have adopted a global metal mass fraction of $Z = 0$. Assuming a global metal mass fraction of $Z = 0.1$, compute what $n_{\rm H}$ would be. [HINT: you might confirm that you can reproduce their result before finalizing your answer].

2. **[25 pts] The Favored Scenario:**

   Per the Discussion section, § 4, the authors interpret the absorbing gas as a multiphase intragroup medium in a small group of galaxies at the redshift of the absorption (the galaxies they reference were reported in an earlier paper). The galaxy IDs, impact parameters, and redshifts (in km s^{-1}) from that paper are presented in Table 1 of this exam.

   (a) [4 pts] Assuming all galaxies have the same mass, compute the line of sight barycenter velocity of the galaxy group. Give your answer in km s^{-1}. What is the redshift of the group barycenter?

   (b) [9 pts] Assuming that the hot absorbing gas observed in O VIII absorption is thermally broadened with a temperature $T = 10^7$ K, compute the FWHM of the line of sight velocity dispersion of the hot gas. Give your and answer in km s^{-1}.

   (c) [10 pts] The provided "blank" diagram shows the line of sight velocity along the horizontal and the impact parameters along the vertical. Using the data provided in Figure 1 and Table 1 of the paper, draw a schematic of the galaxies and the intragroup gas clouds seen in absorption. Draw the Lyα and O VIII absorbing gas clouds as "circularish blobs" with sizes in rough proportion to their line of sight velocity FWHM. For full credit, on your diagram [i] mark and label the line of sight galaxy group barycenter velocity on the line of sight, [ii] sketch and label each galaxy (G1, G2, etc), [iii] sketch and identify/label each gas cloud (A, B, barycenter, etc), [iv] for each Lyα cloud (A, B, etc) indicate/label which ions are observed in absorption, [v] label the cloud(s) that is(are) believed to the shocked gas *and* the gas that is the "hot" gas.

   (d) [2 pts] Based upon the notion of the author's "far side" and "near side" infall model, on your diagram identify the cloud that is physical (spatially) on the observer's side of the line of sight and which is physically on the side opposite the observer.

3. **[20 pts] The Shocked Gas and Cooling Time**

On page 110, the authors state "Adiabatic shocks can provide a compressive trigger, but further radiative cooling is required since adiabatic compression lengthens the cooling time." The authors assume that the shocked gas temperature, T_s, is in the regime where the radiative cooling rate coefficient, $\Lambda(T)$, scales as $\Lambda(T) \propto T^{-1}$. From inspection of the [Fe/H] = 0.1 solar metallicity cooling function (see hand out), this scaling applies in the range $5.4 \leq \log T \leq 6.6$.

(a) [8 pts] Employing the author's expression for the cooling time, $t_{\rm cool}$, and using the cooling curve adopted by the authors, compute the gas total number density, n, at which the cooling time equals the age of the universe, $t_{\rm univ}$, for a shock velocity of $V_s = 300$ km s^{-1}. Express you answer as n_{-4}.

(b) [5 pts] Assuming $T \propto n^{2/3}$ for adiabatic compression, show that $t_{\rm cool} \propto n^{1/3}$ under the author's assumed conditions.

(c) [2 pts] The authors deduce that $n_{-4} \simeq (\delta/500)$ and that $\delta > 500$. What is the definition of δ. Write this definition down in symbolic form and provide a written definition of the terms.

(d) [5 pts] If this deduced density, i.e.,$n_{-4} \simeq 1$, is required in order for the gas to "cool, recombine, and form the observed O VI", what does this imply about the thermal evolution of shocked gas. In your response, consider your answer to part (a) above, and consider the behavior (slope) of the cooling function to guide your answer.

Table 1. Some Possibly Useful Constants

quantity	symbol	value
hydrogen mass	$m_{\rm H}$	1.67×10^{-24} g
oxygen mass	$m_{\rm O}$	$16 m_{\rm H}$
Boltzmann constant	k	1.38×10^{-16} erg K^{-1}
Hubble parameter	$h = H_0/100$	0.71
Critical Density	ρ_c	$1.88h^2 \times 10^{-29}$ g cm^{-3}
age of universe	$t_{\rm univ}$	13.7 Gyr

Table 2. Galaxy Properties

ID	D kpc	$V_{\rm helio}$ km s^{-1}	Sky Direction
G1	650	17,060	East
G2	785	16,650	East
G3	565	17,160	East
G4	400	17,290	West
G5	520	16,240	West

The Astrophysical Journal, 594:L107–L110, 2003 September 10

THE MULTIPHASE INTERGALACTIC MEDIUM TOWARD PKS 2155−304

J. Michael Shull,[1,2] Jason Tumlinson,[3] and Mark L. Giroux[4]

Received 2003 June 30; accepted 2003 July 31; published 2003 August 11

ABSTRACT

We study the cluster of H I and O VI absorption systems and the claimed detection of O VIII absorption from the intergalactic medium at $z \approx 0.0567$, associated with a group of galaxies toward the BL Lac object PKS 2155−304. As measured by spectrographs on the *Hubble Space Telescope*, *Far Ultraviolet Spectroscopic Explorer*, and *Chandra*, this system appears to contain gas at a variety of temperatures. We analyze this multiphase gas in a clumpy-infall model. From the absence of C IV and Si III absorption in the Lyα clouds, we infer metallicities less than 2.5%–10% of solar values. The only metals are detected in two O VI absorption components, offset by ± 400 km s^{-1} from the group barycenter ($cz \approx 16{,}600$ km s^{-1}). The O VI components may signify "nearside" and "backside" infall into the group potential well, which coincides with the claimed O VIII absorption. If the claimed O VIII detection is real, our analysis suggests that clusters of strong Lyα and O VI absorbers, associated with groups of galaxies, may be the "signposts" of shock-heated metal-enriched baryons. Through combined UV and X-ray spectra of H I and O VI, O VII, and O VIII, one may be able to clarify the heating mechanism of this multiphase gas.

Subject heading: intergalactic medium

1. INTRODUCTION

With the development of high-throughput ultraviolet and X-ray spectrographs, we can begin to account for a significant fraction of the low-redshift "missing baryons" (Fukugita, Hogan, & Peebles 1998; Shull 2003) in the intergalactic medium (IGM). Recent surveys by the *Hubble Space Telescope* (*HST*) and the *Far Ultraviolet Spectroscopic Explorer* (*FUSE*) show that 29% ± 4% of the baryons reside in the warm (10^4 K) Lyα forest (Penton, Stocke, & Shull 2003), while 5%–10% lie in the shock-heated (10^5–10^6 K) IGM traced by O VI absorption (Tripp, Savage, & Jenkins 2000). A predicted 30%–40% of the IGM remains to be found in even hotter gas (10^6–10^7 K) through X-ray absorption lines of O VII, O VIII, and perhaps Ne IX (Fang et al. 2002; Nicastro et al. 2002).

The total baryon density is known to 10% accuracy from measurements of light-element nucleosynthesis (D/H) and acoustic oscillations in the cosmic microwave background (CMB). Recent estimates from these techniques yield consistent values for Ω_b, the fractional contribution of baryons to the closure density: $\Omega_b = 0.020 \pm 0.002\,h^{-2}$ (D/H; Burles & Tytler 1998) and $\Omega_b = 0.0224 \pm 0.0009\ h^{-2}$ (CMB; Spergel et al. 2003; Netterfield et al. 2002) for a Hubble constant $H_0 = 100\ h$ km s^{-1} Mpc^{-1}. Even H_0 has become a well-measured parameter, with values of $h = 0.71 \pm 0.08$ (Freedman et al. 2001) from the Cepheid Key Project with *HST*. Using the CMB values, the comoving baryon density is $\rho_b = (4.2 \pm 0.2) \times 10^{-31}$ g cm^{-3} and the hydrogen density is $n_{\rm H} = (1.90 \pm 0.2) \times 10^{-7}$ cm^{-3} for primordial helium abundance $Y_p = 0.244$ by mass.

Numerical simulations of the low-z IGM (Cen & Ostriker 1999; Davé et al. 2001) predict that the gas is distributed nearly equally (30% ± 10% each) in three "phases": (1) warm photoionized gas (10^4 K), (2) warm/hot shocked gas (10^5–10^7 K), and (3) collapsed halos, galaxies, and clusters with much hotter gas ($T > 10^7$ K). The warm phase is observable through UV absorption lines of H I, C III, C IV, Si III, and Si IV, while the warm/hot phase is detectable in O VI (UV) and in X-ray lines of O VII, O VIII, and Ne IX. The warm-hot intergalactic medium (WHIM) is thought to be produced by shock heating during gravitational infall into dark matter filaments coevolving with the rise in cosmic metallicity. These heavy elements are theorized to be expelled from galaxies by tidal stripping (Gnedin 1998) and "starburst winds," as observed by Martin, Kobulnicky, & Heckman (2002). The metals are then assimilated into infalling clumps of IGM. Details of this model remain unclear. Are the heavy elements expelled from galaxies in hot or warm gas? How are the metals mixed with the IGM? What is the extent of their transport? Addressing these issues requires detecting and correlating many warm and hot IGM absorbers.

In this Letter, we provide clear evidence for multiphase IGM toward the BL Lac object PKS 2155−304. This gas is associated with a small group of galaxies at $z \approx 0.0567$ and a cluster of seven strong Lyα absorbers (Shull et al. 1998) at velocities $cz = 16{,}283$–$17{,}570$ km s^{-1}. This environment exhibits the diffuse warm phase (Lyα, Lyβ, Lyγ), the shocked (WHIM) phase (O VI), and unconfirmed evidence (O VIII) for much hotter virialized gas residing at the bottom of the group's gravitational potential well.

In § 2, we describe our *FUSE* and *HST* observations of these absorbers in H I and O VI (and limits on C IV and Si III) and compare them to the claimed O VIII absorption. In § 3 we examine the absorber kinematics for the possibility of nearside/backside infall and ionization-state (O VI/O VIII) consistency. We conclude in § 4 with a discussion of an infall model that may be consistent with large-scale structure in this group. In this picture, the H I and O VI absorbers arise from clumps of gas falling at 200–400 km s^{-1} relative to a much hotter ($10^{6.5}$–$10^{7.0}$ K) substrate that could be detectable in O VII or O VIII absorption. The metallicities may range from 0.02 to 0.1 solar. All the phases predicted by simulations may be present in this group, suggesting that clusters of strong Lyα and

---

[1] Center for Astrophysics and Space Astronomy, Department of Astrophysical and Planetary Sciences, University of Colorado, Campus Box 391, Boulder, CO 80309; mshull@casa.colorado.edu.

[2] Also at JILA, University of Colorado, and National Institute of Standards and Technology.

[3] Department of Astronomy and Astrophysics, University of Chicago, 5640 South Ellis Avenue, Chicago, IL 60637; tumlinso@oddjob.uchicago.edu.

[4] Department of Physics and Astronomy, East Tennessee State University, Box 70652, Johnson City, TN 37614; giroux@polar.etsu.edu.

O vi absorbers associated with groups of galaxies may be the "signposts" of shock-heated metal-enriched baryons.

2. OBSERVATIONS

In *HST* Cycle 9, we obtained new data from the Space Telescope Imaging Spectrograph (STIS) Echelle (E140M) with 10 orbits (PID 8125, 28.5 ks) and compared the absorber velocities to those in a small group of galaxies containing four large H i galaxies and one dwarf seen with the Very Large Array (see Fig. 3 in Shull et al. 1998). The PKS 2155−304 sight line passes near the center of this group, none of these galaxies lies closer than 400 kpc to the sight line, and no other dwarf galaxies were seen down to $m_B \approx 19$. The galaxy one-dimensional velocity dispersion is $\sigma_{\rm gal} = 325$ km s^{-1}, and the Lyα velocity dispersion is $\sigma_{{\rm Ly}\alpha} = 740$ km s^{-1}. We estimate the galaxy overdensity as $\delta \sim 100$, based on the group of five galaxies.

We also observed PKS 2155−304 with *FUSE* (Moos et al. 2000) in three visits on 1999 October 23–24 (P1080701, $t_{\rm exp} = 19.2$ ks, and P1080705, $t_{\rm exp} = 38.6$ ks) and 2001 June 18 (P1080703, $t_{\rm exp} = 65.4$ ks). All data were calibrated with CALFUSE, version 2.2.1. We base most of our analysis on the second visit, which obtained data for all of the *FUSE* detectors, whereas the earlier visits occurred before the SiC and LiF channels (Sahnow et al. 2000) were aligned. For the LiF1a segment (1000–1084 Å), we roughly tripled the amount of available data by co-adding night-only reductions of the three observations. This method recovered the redshifted Lyγ absorption (1027.6 and 1028.0 Å) from below O i airglow emission (1025.76 and 1026.47 Å). We applied small wavelength offsets ($\leq$0.05 Å) to the *FUSE* data to align narrow interstellar lines and place the *FUSE* and STIS data on a common velocity scale set by Galactic 21 cm emission.

The claimed X-ray detection of O viii absorption (Fang et al. 2002) with 4.5 σ significance was made with the *Chandra* Low Energy Transmission Grating Spectrometer (LETG). However, the redshifted O viii absorber is not seen near 20 Å in the spectrum taken by the *X-Ray Multi-Mirror* (*XMM*) mission (see Fig. 1 and Table 1 in Rasmussen, Kahn, & Paerels 2003). Although the *XMM* velocity resolution is poorer than that of *Chandra*/LETG, the *XMM* data have a high signal-to-noise ratio (S/N) and detect oxygen absorption at $z = 0$ with equivalent widths 16.3 ± 3.3 mÅ (O viii, 5.7 σ significance) and 9.0 ± 2.7 mÅ (O vii, 8 σ significance). The nonconfirmation of the $z = 0.0567$ O viii absorption remains a puzzle.

Figure 1 shows a velocity overlay of the Lyα, Lyγ, O vi, and O viii absorbers between cz = 15,000 and 20,000 km s^{-1}. The detected lines and their properties are summarized in Table 1; the three strong Lyα absorbers are labeled A, B, and C for clarity. We detect Lyβ at 16,243 km s^{-1} (A), but Lyβ lines at 16,973 (B) and 17,110 km s^{-1} (C) are severely blended with the N ii λ1084 interstellar line. We detect Lyγ in components B and C, but we derive a large error on their equivalent width because of continuum placement uncertainty. We also detect O vi in components A and C, at 16,243 and 17,144 km s^{-1}.

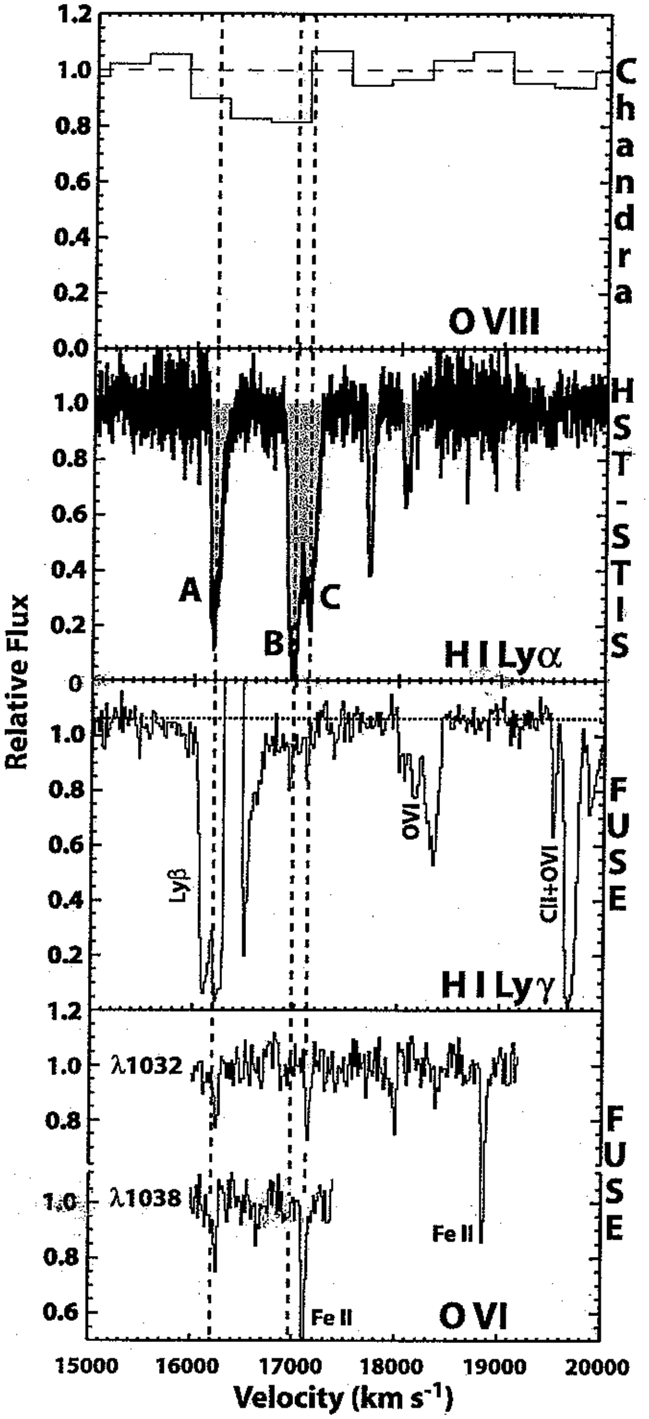

FIG. 1.—Absorption lines of H i (Lyα from *HST*/STIS, Lyγ from *FUSE*), O vi 1032/1038 (*FUSE*), and claimed detection of O viii with *Chandra* (Fang et al. 2002) toward PKS 2155−304. The three strongest Lyα absorbers are labeled (A, B, and C; see Table 1). We detect O vi in the 16,243 km s^{-1} (A) and 17,144 km s^{-1} (C) absorbers, and Lyγ in B and C absorbers; claimed O viii absorption is offset by ~400 km s^{-1} from Lyα and O vi (*vertical dotted lines*). Interstellar lines (Lyβ, C ii, and O vi) are labeled in the third panel. The bottom curve in the fourth panel shows O vi 1038 offset from O vi 1032. The Fe ii line shows an asymmetric profile that suggests the presence of O vi 1038 at 17,140 km s^{-1}, but blending precludes an accurate measurement.

3. INTERPRETATION OF THE SPECTRA

With our new *HST*/STIS E140M data, we can derive more accurate column densities and metallicities for the strong Lyα absorbers. In our previous study (Shull et al. 1998) at 20 km s^{-1} (*HST*/Goddard High Resolution Spectrograph) resolution, we estimated $N_{\rm H\,I} = (3\text{–}10) \times 10^{14}$ cm^{-2} for the blended B and C components at $z \approx 0.0567$. There, we set a metallicity limit $Z < 0.003\ Z_\odot$ from the absence of Si iii and C iv absorption. At the higher S/N and better spectral resolution of the STIS/E140M, together with *FUSE* measurements of Lyγ, the derived H i columns decreased considerably. The integrated Lyα optical depths give N(H i) = 1.0, 2.2, and 0.94 × 10^{14} cm^{-2}, respec-

TABLE 1

PKS 2155−304 IGM Absorption Lines

Line	Velocity (km s^{-1})	W_λ (mÅ)	ΔV^a (km s^{-1})
H i Lyα (A)	16185 ± 5	331 ± 12	75 ± 8
H i Lyα (B)	16974 ± 5	495 ± 10	76 ± 5
H i Lyα (C)	17147 ± 5	353 ± 8	110 ± 10
H i Lyβ (A)	16243 ± 10	85 ± 10	92 ± 17
H i Lyγ (B)	16936 ± 10	16 ± 4	<30
H i Lyγ (C)	17109 ± 10	13 ± 3	<30
H i Lyδ^b	...	<12	<30
O vi λ1032 (A)	16243 ± 10	37 ± 7	35 ± 10
O vi λ1038 (A)	16252 ± 10	25 ± 5	30 ± 10
O vi λ1032 (C)	17144 ± 10	44 ± 6	40 ± 10
O vi λ1038 (C)	17116 ± 10	Fe ii blend	...
O viii λ18.969	16624 ± 237	$14.0^{+7.3}_{-5.6}$	<1380
C iii λ977^b	...	<10	...
C iv λ1548^b	...	<12	...
Si iii λ1206^b	...	<6	...

[a] FWHM from STIS/*FUSE* profile fitting or by converting *Chandra* line width of σ(O viii) < 0.039 Å (Fang et al. 2002). The Doppler parameter $b_{\rm Dopp}$ = FWHM/[2(ln 2)$^{1/2}$].

[b] Upper limit at 4 σ significance.

tively, for absorbers at 16,185, 16,974, and 17,147 km s^{-1}, consistent with the observed Lyγ strengths.

We still did not detect any Si iii λ1206 or C iv λ1548 absorption at the Lyα velocities (Table 1). The 6–12 mÅ equivalent width limits correspond to N(C iv) < 2.9 × 10^{12} cm^{-2} and N(Si iii) < 2.7 × 10^{11} cm^{-2}. As described in Shull et al. (1998), we assume that the absorption arises in a uniform slab of gas photoionized by the metagalactic radiation background, with spectral shape for a background dominated by active galactic nuclei with intrinsic spectral index of α = 1.8 modified by IGM absorption (Shull et al. 1999). The ionization correction (conversion from C iv/H i to [C/H]) depends only on the ionization parameter, log $U \propto I_0/n_{\rm H}$, where I_0 is the specific intensity at 1 ryd and $n_{\rm H}$ is the volume density of the gas. For $-2.0 <$ log $U < -0.5$, the metallicity upper limit from C iv/H i ranges between 0.025 and 0.10 of the solar abundance in the CLOUDY photoionization code, (C/H)$_\odot$= 3.55 × 10^{-4} (Grevesse & Noels 1993). A full discussion of the parameter dependence of the metallicity estimate appears in a subsequent paper.

The two detected O vi systems have column densities of N(O vi) = (2.8 ± 0.5) × 10^{13} cm^{-2} (A) and (3.3 ± 0.5) × 10^{13} cm^{-2} (C), assuming a linear curve of growth. At the temperature (log $T_{\rm O\,VI}$ = 5.45) of maximum ionization abundance ($b_{\rm O\,VI}$ = 17 km s^{-1}), the stronger O vi λ1032 lines in both components would still be unsaturated. We identify these two O vi absorbers with Lyα systems at 16,185 (A) and 17,147 km s^{-1} (C). No O vi is seen in the 16,974 km s^{-1} (B) absorber. The O vi lines are the only metals yet detected in these absorbers, but their metallicity is uncertain, owing to an indeterminate ionization state and thermal phase (see Savage et al. 2002). If the O vi arises in photoionized gas, its column density and limits on C iv imply log $U > -0.8$, for C/O in a solar abundance ratio of 0.50 ± 0.07 (Allende Prieto, Lambert, & Asplund 2002).

If the ionizing background has $I_0 \approx 10^{-23}$ ergs cm^{-2} s^{-1} Hz^{-1} sr^{-1} (Shull et al. 1999), the density constraint is $n_{\rm H} < 10^{-5.6}$ cm^{-3}, and the corresponding line-of-sight extent of the gas is $D >$ 1.1 Mpc, comparable to the extent of the galaxy group. We believe that this low-density large-absorber model is highly unlikely. Multiple absorbers of this extent could not fit within the 1 Mpc volume of the group, without undergoing collisions and shredding. However, if the O vi arises in collisionally ionized gas, the requirement that the gas be so rarefied no longer holds. In addition, the fraction of O vi in collisional ionization equilibrium peaks at $T \sim 10^{5.5}$ K, and it is tempting to associate the O vi with the WHIM. The tentative detection of O viii absorption makes collisionally ionized O vi still more compelling. The claimed strength of the X-ray feature (Fang et al. 2002) requires log N(*O* viii) ≈ 16.0 ± 0.2, which could represent hot gas at the group barycenter. However, redshifted O viii absorption was not confirmed by *XMM*, nor has O vii absorption at z = 0.0567 been detected (Nicastro et al. 2002).

4. DISCUSSION

In order to understand the cluster of PKS 2155−304 absorbers at $z \approx 0.0567$, one must resort to a multiphase model. The H i, O vi, and O viii systems are unlikely to coexist, owing to kinematic offsets and physical considerations. For example, the claimed O viii absorption centroid (16,624 ± 237 km s^{-1}) appears to differ from the observed H i and O vi absorbers (A, B, and C components). Also, the observed Lyγ line widths (FWHM ≤ 30 km s^{-1}) rule out H i temperatures greater than 20,000 K. The measured O vi line widths (40 ± 10 km s^{-1} FWHM) make it unlikely, although marginally possible within errors, for O vi and O viii to exist at the same temperature, log $T \approx 6.25 \pm 0.1$, where (O vi/O viii) ≈ 6 × 10^{-3} in collisional ionization equilibrium (Sutherland & Dopita 1993). However, we discount this scenario, because of the observed velocity offsets (∼400 km s^{-1}). For similar reasons, the strong H i absorbers cannot coexist with the hot O viii. At the high temperatures needed to ionize O viii collisionally, the H i ionization fraction would be too small to be detected.

Therefore, we favor a more complex scenario in which the H i and O vi absorbers arise in clumps of gas falling into a small-group potential. Any hot gas, visible in O vii or O viii, would then exist at the barycenter of the group (16,600 km s^{-1}), which would be consistent with the kinematic offsets. If this model is correct, the two O vi absorbers (A and C) would arise from clumps undergoing backside and nearside infall, respectively. Because production of collisionally ionized O vi requires shock velocities $V_s \geq 130$ km s^{-1} (Shull & McKee 1979; Dopita & Sutherland 1996), the infall model has consequences for which Lyα absorbers contain associated O vi. In particular, the absence of detectable O vi in the strongest Lyα system (B) may be a result of a low relative velocity between the infalling H i clump and the substrate. From Figure 1, one sees that O vi is present in the H i absorber at 17,147 km s^{-1}, located approximately 170 km s^{-1} redward. Thus, one might speculate that these two blended Lyα absorbers, one with and one without O vi, represent shocked and unshocked gas.

In the clumpy-infall model, the relative velocity between the two O vi components and the group barycenter is ∼400 km s^{-1}, which would produce a postshock temperature of ∼2 × 10^6 K, similar to that (2.5 × 10^6 K) at which the observed O vi and claimed O viii would coexist in collisional ionization equilibrium. The cooling time of such gas is

$$t_{\rm cool} = \frac{(20\ {\rm Gyr})T_{6.5}}{n_{-4}\Lambda_{-23}}, \qquad (1)$$

where $n_{-4} = n_{\rm H}/(10^{-4}\ {\rm cm^{-3}})$ and $T_{6.5} = (T/10^{6.5}\ {\rm K})$. Here, Λ_{-23} is the radiative cooling rate coefficient in units of 10^{-23} ergs cm^3 s^{-1}, typical of gas at 10$^{6.5}$ K with 0.1 solar metallicity (Sutherland & Dopita 1993). In the range $5.0 < \log T < 7.0$, $\Lambda(T) \propto T^{-1}$, so $t_{\rm cool}$ is longer than the age of the universe, unless the gas temperature can be decreased ($T_{6.5} \ll 1$) or the density increased ($n_{-4} \gg 1$). Through shock compression and cooling, the cooling will accelerate as $\Lambda(T)$ moves toward its $10^{5.3}$ K peak.

We can relate the hydrogen density to the cosmological overdensity δ by

$$n_{\rm H}(z) = (1.90 \times 10^{-7}\ {\rm cm}^{-3})(1+z)^3 \frac{\Omega_b h_{70}^2}{0.046}(1+\delta). \qquad (2)$$

At the redshift ($z_a = 0.0567$) of the strong absorbers, we have $n_{-4} \approx (\delta/500)$. If the infalling gas is shocked to $T_s = (1.24 \times 10^6\ {\rm K})(V_s/300\ {\rm km\ s^{-1}})^2$ to form the WHIM phase, it must acquire a fairly high density ($\delta > 500$ at $z \approx 0.1$) in order to cool, recombine, and form the observed O VI. Adiabatic shocks can provide a compressive trigger, but further radiative cooling is required, since adiabatic compression lengthens the cooling time [$t_{\rm cool} \propto n^{1/3}$ for $T \propto n^{2/3}$ and $\Lambda(T) \propto T^{-1}$]. Lower velocity shocks, $V_s \approx 200$ km s^{-1}, would cool more rapidly, with temperatures near the peak of the cooling curve.

Two additional issues concern the ratios of C IV, O VI, and H I. In the two detected O VI absorbers, (C IV/O VI) $< 10^{-1.1}$, whereas models of radiatively cooling gas (Dopita & Sutherland 1996; Indebetouw & Shull 2003) find (C IV/O VI) $\approx$ 0.1–0.2. Where is the C IV? Is the cooled recombined layer truncated in the hot-gas environment? Similarly, we do not understand the wide variation in [N(H I)/N(O VI)] ≈ 0.1–10 among other IGM absorbers (Shull 2003). The production of shocked O VI requires *relative* velocities above ~150 km s^{-1} and O/H abundances above a few percent solar. However, the production mechanism of O VI remains unclear (Sembach et al. 2003). While shock heating is the preferred mechanism, other processes have been proposed involving interfaces between hot substrates and moving clouds—thermal conduction, shear instabilities, and turbulent mixing (see Indebetouw & Shull 2003 for a review). These processes all have problems explaining the observed components, N(O VI) $\approx 3 \times 10^{13}$ cm^{-2}. Each conductive interface typically produces N(O VI) ~ 10^{13} cm^{-2}, while shock heating requires supersonic flow and depends on the Mach number cubed. If $T_{\rm hot} \approx 10^{6.4}$ K (adiabatic sound speed $c_s \approx 240$ km s^{-1}), infalling clumps at 300–400 km s^{-1} have Mach numbers of just 1.25–1.67.

Resolving the O VI heating paradox may require understanding the cloud-substrate interfaces at a deeper level. Alternatively, if the O VIII absorption turns out to be nonexistent, a virialized hot substrate may not have formed yet. Intragroup gas at $T < 10^6$ K would produce sufficient shock heating, and the observed O VI absorption may arise from the interactions of infalling clumps with metals in an intragroup medium injected from the galaxies. With combined UV and X-ray spectra, one may be able to distinguish among these processes through the amount of shock heating and the relative abundances of O VI, O VII, and O VIII.

This work is based on data obtained for the Guaranteed Time Team by the NASA-CNES-CSA *FUSE* mission operated by Johns Hopkins University. Financial support to US participants has been provided by NASA contract NAS5-32985. We were also supported by grants GO-08571.01-A from the Space Telescope Science Institute and NAG5-7262 from NASA/LTSA. We thank Taotao Fang for providing the *Chandra* spectrum that appears in Figure 1 and John Stocke and Bill Blair for helpful discussions.

REFERENCES

Allende Prieto, C., Lambert, D. L., & Asplund, M. 2002, ApJ, 573, L137
Burles, S., & Tytler, D. 1998, ApJ, 495, 80
Cen, R., & Ostriker, J. P. 1999, ApJ, 519, L109
Davé, R., et al. 2001, ApJ, 552, 473
Dopita, M. A., & Sutherland, R. S. 1996, ApJS, 102, 161
Fang, T., Marshall, H. L., Lee, J. C., Davis, D. S., & Canizares, C. R. 2002, ApJ, 572, L127
Freedman, W. L., et al. 2001, ApJ, 553, 47
Fukugita, M., Hogan, C. J., & Peebles, P. J. E. 1998, ApJ, 503, 518
Gnedin, N. Y. 1998, MNRAS, 294, 407
Grevesse, N., & Noels, A. 1993, in Origin of the Elements, ed. N. Prantzos, E. Vangioni-Flam, & M. Cassé (Cambridge: Cambridge Univ. Press), 15
Indebetouw, R., & Shull, J. M. 2003, ApJ, submitted
Martin, C. L., Kobulnicky, H. A., & Heckman, T. M. 2002, ApJ, 574, 663
Moos, H. W., et al. 2000, ApJ, 538, L1
Netterfield, C. B., et al. 2002, ApJ, 571, 604
Nicastro, F., et al. 2002, ApJ, 573, 157
Penton, S. V., Stocke, J. T., & Shull, J. M. 2003, ApJ, submitted
Rasmussen, A., Kahn, S. M., & Paerels, F. 2003, in The IGM/Galaxy Connection, ed. J. L. Rosenberg & M. E. Putman (Dordrecht: Kluwer), 109
Sahnow, D. J., et al. 2000, ApJ, 538, L7
Savage, B. D., Sembach, K. R., Tripp, T. M., & Richter, P. 2002, ApJ, 564, 631
Sembach, K. R., et al. 2003, ApJS, 146, 165
Shull, J. M., 2003, in The IGM/Galaxy Connection, ed. J. L. Rosenberg & M. E. Putman (Dordrecht: Kluwer), 1
Shull, J. M., & McKee, C. F. 1979, ApJ, 227, 131
Shull, J. M., Penton, S. V., Stocke, J. T., Giroux, M. L., van Gorkom, J. H., Lee, Y. H., & Carilli, C. 1998, AJ, 116, 2094
Shull, J. M., Roberts, D., Giroux, M. L., Penton, S. V., & Fardal, M. A. 1999, AJ, 118, 1450
Spergel, D. N., et al. 2003, ApJ, in press (astro-ph/0302209)
Sutherland, R. S., & Dopita, M. A. 1993, ApJS, 88, 253
Tripp, T. M., Savage, B. D., & Jenkins, E. B. 2000, ApJ, 534, L1

SOLUTIONS CUME 371 April 21 2012
Churchill

1a] 4pts $\Omega_b = \frac{\rho_b}{\rho_c}$ 2pts

ρ_b = present day (co-moving) density of baryons 1pt

ρ_c = critical present day density of universe 1pt

1b] 5pts $f_b = \frac{\Omega_b}{\Omega_m} = \frac{\rho_b}{\rho_m}$ 2pts

$\Omega_b = 0.02h^{-2} = 0.02(0.71)^{-2} = \boxed{0.039}$ 2pts

$\Omega_m = 0.27$ (given)

$\therefore \quad f_b = \frac{0.039}{0.27} = \boxed{0.15}$ 1pt

15% of matter is baryonic

1c] 4pts $\rho_{proper} = \rho_{comoving}(1+z)^3$ 2pts

$\rho_{proper}(z=0) = \rho_{comoving} = \boxed{\underset{\text{given}}{4.2 \times 10^{-31}}\ \text{g cm}^{-3}}$ 1pt

$\rho_{proper}(z=3) = \rho_{coming}(1+3)^3 = 4^3 \rho_{comoving}$

$= \boxed{2.7 \times 10^{-29}\ \text{g cm}^{-3}}$ 1pt

1d] 7pts $\left.\begin{array}{l} \rho_b = \frac{m_H}{X} n_H \\ \boxed{n_H = \frac{X}{m_H}\rho_b} \end{array}\right\}$ 2pts

$X + Y + Z = 1$

$Z = 0.1$

$\therefore \quad X = 1 - Y - Z = \boxed{0.656}$ } 3pts

$\rho_b = 4.2 \times 10^{-31}\ \text{g cm}^{-3}$ given

$Y = 0.244$ given

$\left.\begin{array}{l} \therefore \quad n_H = \frac{0.656}{1.67 \times 10^{-24}}(4.2 \times 10^{-31}) \\ \boxed{= 1.65 \times 10^{-7}\ \text{cm}^{-3}} \end{array}\right\}$ 2pts

2a] 4pts

$$V_{bary} = \frac{\sum m_i v_i}{\sum m_i} \quad m_i = m_{gal} \longrightarrow \underbrace{V_{bary} = \frac{1}{5}\sum_{i=1}^{5} v_i}_{1pt} = \underbrace{\boxed{16,880 \text{ km/s}}}_{1pt}$$

redshift of barycenter

$$\underbrace{V = cz}_{1pt} \qquad z = \frac{16,8800}{3\times10^5} = \underbrace{\boxed{0.056}}_{1pt}$$

2b] 9pts $T = 10^7$ given $m_O = 16 m_H$ given in Table 2 of cume.

assume Gaussian velocity dispersion $f(v) = \frac{1}{\sqrt{2\pi}\sigma} \cdot \exp\left\{-\frac{\Delta v^2}{2\sigma^2}\right\}$

also $f(v) \propto \exp\left\{-\frac{m \Delta v^2}{2kT}\right\}$

$$\therefore \quad \underbrace{\sigma = \frac{1}{\sqrt{2}}\sqrt{\frac{2kT}{m}}}_{2pts}$$

ASIDE NOTE

[we call $b = \sqrt{\frac{2kT}{m}}$ the Doppler b parameter

$\therefore \quad b = \sqrt{2}\sigma$]

$$\left.\begin{aligned} &\text{FWHM} = 2\sqrt{2\ln 2}\cdot\sigma \\ \therefore\ &\text{FWHM} = 2\sqrt{\ln 2}\sqrt{\frac{2kT}{m}} = 2\sqrt{\ln 2}\cdot b \end{aligned}\right\} \underline{3pt} \text{ (any form)}$$

$$\left.\begin{aligned} &b = \sqrt{\frac{2kT}{m}} = \left\{\frac{2(1.38\times10^{-16})(10^7)}{16(1.67\times10^{-24})}\right\}^{1/2} = 102 \text{ km s}^{-1} \\ &\qquad\uparrow \\ &m_O = 16 M_H \\ &\text{(oxygen)} \\ &\therefore \boxed{\text{FWHM} = 169 \text{ km s}^{-1}} \end{aligned}\right\} \underline{4pts}$$

FYI $2\sqrt{2\ln 2} = 2.35$

2c [10 pts] ← see Diagram

2d [2pts] ← see Diagram

for "near side infall" the cloud must have a recessional (line of sight) velocity greater than the velocity of the group barycenter. This would be cloud "C" (which is to the right of the group on the velocity axis of the diagram!)

1pt

for "far side infall" the cloud must have a line of sight velocity smaller than the velocity of the group barycenter. This is Cloud "A" (which is to the left of the group on the velocity axis of the diagram!)

1pt

[no explantion was required, only proper labelling of the clouds]

Velocity - Impact Parameter Space.
[NOT PHYSICAL SPACE on X-axis]

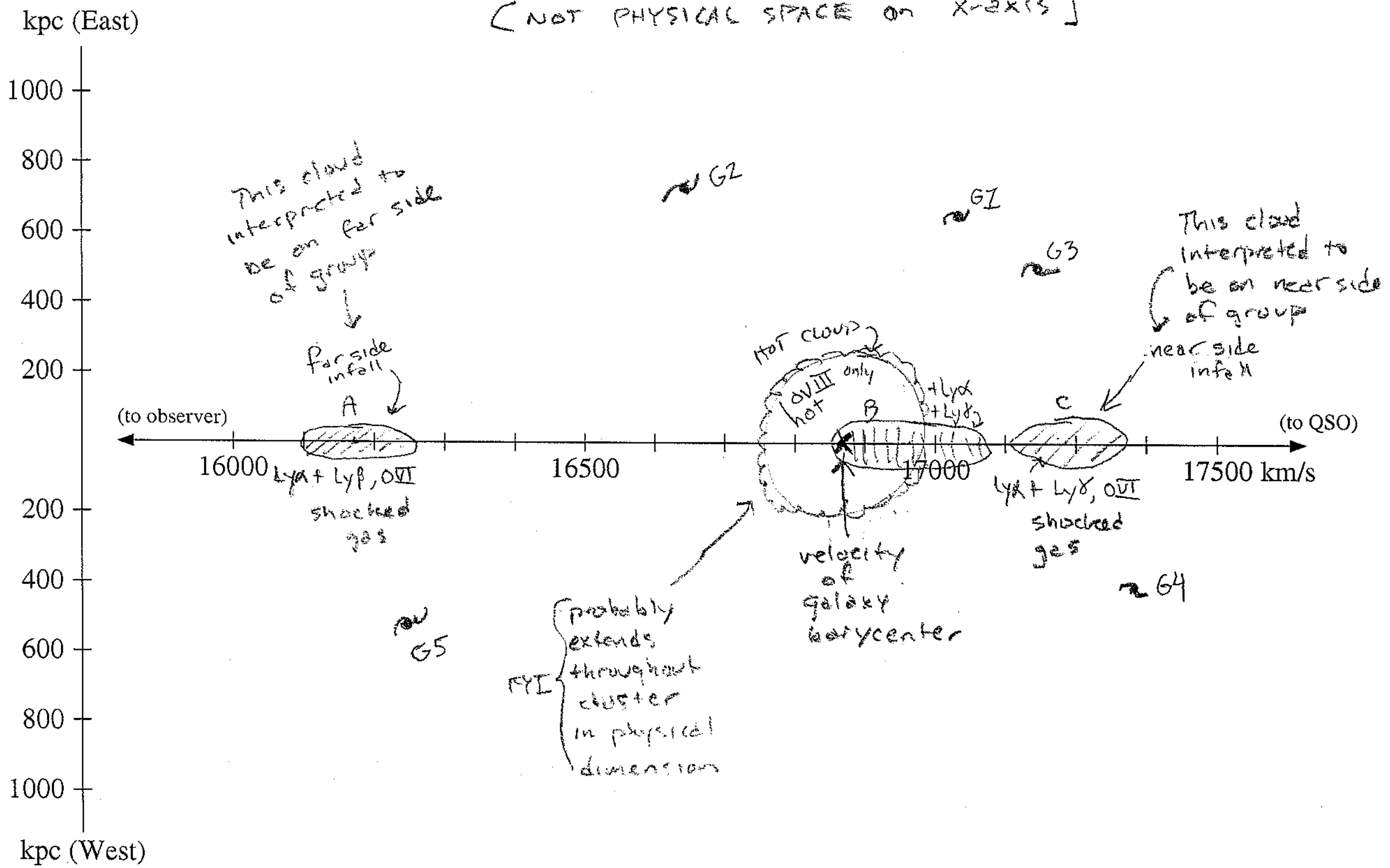

3a] 8pts $V_{shock} = 300\ km\ s^{-1}$ given

from paper $T_{shock} = 1.24 \times 10^6 \left(\frac{V_{shock}}{300\ km/s}\right)^2 = 1.24 \times 10^6\ K$ } 2pts

$T_6 = 0.39$

$$t_{cool} = \frac{20\ T_6}{n_{-4}\ \Lambda_{-23}}$$

want $t_{cool} = t_{univ} = 13.7$ Gyr

$$n_{-4} = \frac{20}{t_{univ}} \cdot \frac{T_6}{\Lambda_{-23}}$$

authors use [Fe/H] = 0.1 cooling curve. (see next page) →

using $\log T_{shock} = 6.1$

reading from Λ curve, $\Lambda = 10^{-22.7} \rightarrow \Lambda_{-23} = 2$ } 2pts

$$\therefore\ n_{-4} = \frac{20}{13.7} \cdot \frac{0.39}{2} = \boxed{0.285}$$ } 4pts ← includes setting $t_{cool} = t_{univ}$

3b] 5pts given $T \propto n^{2/3}$ $\Lambda \propto T^{-1}$

$$t_{cool} \propto \frac{T}{n\Lambda} = \frac{n^{2/3}}{n \cdot n^{-2/3}} = \frac{n^{4/3}}{n} = n^{1/3}$$ } 5pts

FYI { in adiabatically compressed gas, cooling time increases with density in range $5.4 < \log T < 6.6$!
– as gas gets compressed and heats, it cannot cool

ating (or cooling)
the electron gas.
tio of the thermal
ns that are being
given by:

, (7.2)

$_\gamma$ is the scattering
of the photon, $h\nu$,
gy as $E = \gamma m_e c^2$,
tic) Klein–Nishina

$$q) - \frac{(1+3q)}{(1+2q)^2} \Bigg\} , \quad (7.3)$$

(7.4)

^{2}, (7.5)

ss section. In the
here,

(7.6)

asymptotic forms:

(7.7)

appears explicitly
.

nsity cooling plas-
and/or the plasma
Compton terms can
only the ground
to any appreciable
epend on two-body
e written as

(7.8)

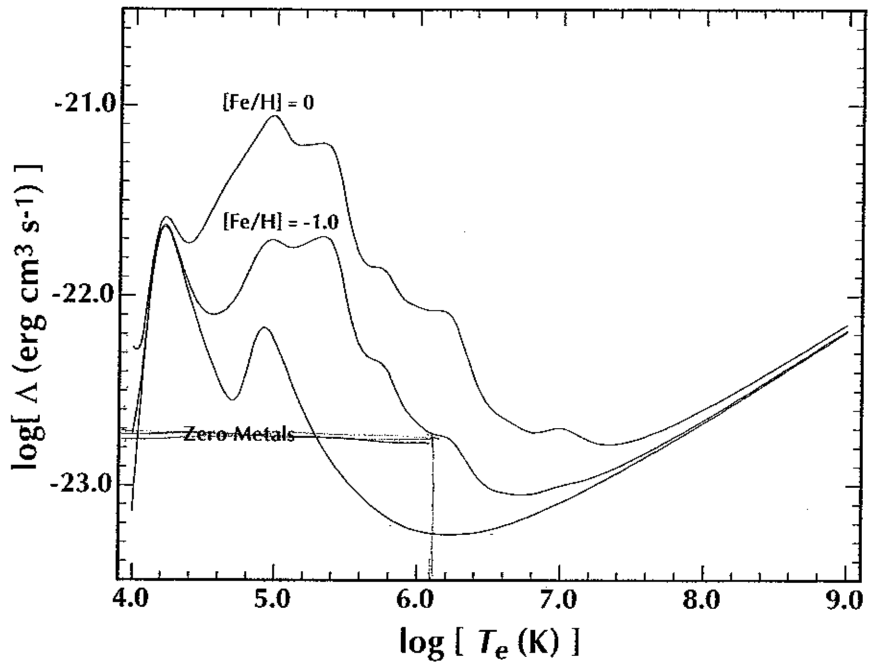

Fig. 7.1. The collisional-ionization cooling function as a function of metallicity. At zero "metals" (elements heavier than helium), the peaks due to hydrogen and helium are apparent, while those of carbon, oxygen, neon, silicon, and iron become apparent in the other curves (after Sutherland & Dopita, 1993).

where n is the total density of atoms and ions per unit volume. Writing the heat loss in this form allows the density dependence to be separated from the temperature dependence. The *cooling function* of the plasma (in units of erg cm^{3}s^{-1}) is therefore

$$\Lambda(T_e, Z_A) = \Lambda_{\text{line}} + \Lambda_{\text{coll}} - \Lambda_{\text{rec}} + \Lambda_{\text{cont}}. \quad (7.9)$$

Figure 7.1 shows the cooling function derived for collisional ionization equilibrium conditions as a function of the heavy element abundance, from Sutherland & Dopita (1993).

When only hydrogen and helium are present, the cooling function is dominated by the collisional excitation of excited states in H^0 and He^0 for the temperature range $\log(T_e) \lesssim 4.6$. For higher temperatures, up to $\log(T_e) \sim 5.6$, collisional excitation of He^+ dominates the cooling. At still higher temperatures, electron free-free cooling is dominant. The X-ray spectrum of such a free-free dominated plasma is very simple, and is given by the sum of the free-free emissivity of all the ions, i of element, el present, from (6.22) and (6.23), 3c] 2pts

$$\delta = \frac{\Delta\rho}{\bar{\rho}} \quad 1pt$$

$$\Delta\rho = \rho - \bar{\rho}$$

$\bar{\rho}$ = mean density

δ expressed the fraction overdensity or underdensity of a region of space as compared to the mean density

3d] 5pts.

1. the gas has density greater than the density at which the cooling time is equal to τ_{univ} i.e. $n_{-4} = 1$ is greater than $n_{-4} \approx 0.28$ for this T } from 3a
2pts

2. In adiabatic compressed gas the cooling time goes as $\tau_{cool} \propto n^{1/2}$; therefore the cooling time increases with density at this T } from 3b
2pts

taken together this implies that during adiabatic compression, the shocked gas should never cool to the point that OVI is observed.
1pt

∴ as author state, another cooling mechanism must be in place, which they identify as radiative cooling →

this also implies that the OVI is being observed post-shocking.